

Cationic Thionin Blue in the Channels of Zeolite Mordenite: A Single-Crystal X-ray Study

Petra Simoncic,^{*,†} Thomas Armbruster,^{*,†} and Phil Pattison[‡]

Laboratorium für chemische und mineralogische Kristallographie, University of Bern, Freiestrasse 3, CH-3012 Bern, Switzerland and Swiss Norwegian Beamline (SNBL), ESRF, Grenoble, France

Received: June 22, 2004; In Final Form: August 25, 2004

Single crystals of self-synthesized mordenite–Na were used for incorporation of the cationic dye molecule thionin blue ($C_{12}H_{10}N_3S^+$). The planar organic molecule ($7.5 \times 15 \text{ \AA}$), which fits into the large 12-membered ring channel of mordenite, was incorporated by ion-exchange replacing extraframework Na^+ cations. Deep blue thionin-exchanged mordenite crystals were chemically analyzed by electron microprobe yielding the composition $Na_{5.5}Thionin_{0.4}Si_{42.02}Al_{5.88}O_{96} \times nH_2O$ indicating that the large 12-membered ring channels of mordenite are less than half-filled by dye molecules. X-ray data collection of thionin-loaded mordenite single crystals was performed at 120 K with synchrotron radiation ($\lambda = 0.80000 \text{ \AA}$) using the single-crystal diffraction line at the Swiss Norwegian Beamline, SNBL (ESRF, Grenoble) where diffracted intensities were registered with an MAR image plate. The structure of thionin–mordenite–Na was refined in the monoclinic space group Cc converging at $R1 = 5.53\%$. Optical microscopy of dye-loaded mordenite single crystals using plane-polarized light showed striking pleochroism due to anisotropic light absorption caused by the preferred orientation of the molecule's transition-dipole moment. Corresponding anisotropic phenomena were also observed by fluorescence microscopy. Four low populated thionin sites were located in the large mordenite channel. Determined $S \cdots O$ ($2.97(1)–3.18(1) \text{ \AA}$), $C \cdots O$ ($3.11(1)–3.36(2) \text{ \AA}$) and $N \cdots O$ ($3.04(1)–3.20(1) \text{ \AA}$) distances from the dye molecule to the channel wall indicate electrostatic interaction with the framework. The molecules are arranged slightly inclined within the large 12-membered ring channels showing significant occupational disorder along the channel axis. The flat geometry of the thionin molecule enables a rotation of about 12° in each direction causing distinct disorder within the channel cross section.

Introduction

Zeolites are characterized by open framework systems building channels and cavities with free apertures up to 13 \AA in diameter. These channel systems are crucial for the properties and applications of zeolites, for example, the well-established use as catalysts or molecular sieves. However, new and more sophisticated functions of zeolites in photochemistry emerged in the past decade. Host–guest systems built by photochromic, luminescent dyes intercalated into zeolites allow various applications as microlasers, pigments, optical switches, or artificial antenna systems.^{1–3} The well-defined internal structure of the zeolite framework provides the organization and arrangement of incorporated chromophores in terms of thermal or mechanical stabilization. Various zeolites with suitable channel dimensions, such as zeolite L,^{1,2} $AlPO_4$ -5,^{4,5} zeolite Y,⁶ and also mesoporous materials such as MCM-41,⁷ have successfully been used for formation of these host–guest systems. Monomeric organized dyes in zeolites have striking optical effects such as anisotropic light absorption or luminescence and fluorescence phenomena caused by the preferred orientation of the transition-dipole moment of the dye molecules.

Research on zeolite guest–host systems is generally focused on three areas: (1) incorporation processes of dye molecules into zeolites, (2) investigation of the energy-transfer mechanism, and (3) geometrical characterization of the dyes within the zeolite framework.

Three different methods for dye incorporation have been established: (1) Ion exchange: Cationic dye molecules such as oxonine, pyronine, thionin, or methylene blue can be encapsulated into zeolites by ion exchange in aqueous solution where extraframework metal cations normally filling the zeolite channels are replaced by the charged dyes. (2) Vapor phase deposition: Neutral chromophores such as fluorenone, naphthalene, or anthracene can be inserted into a zeolite framework bringing the dyes into gas phase. Incorporation by gas phase requires a preceding dehydration of the zeolite because H_2O molecules block the pathway for the entering molecules. (3) In-situ encapsulation during zeolite synthesis where the photochromic molecules are added to the synthesis starting materials and encapsulated during crystal growth.

Energy-transfer mechanisms in dye-modified zeolites were mainly investigated by the group of Calzaferri applying UV/vis, fluorescence microscopy, and IR/Raman spectroscopy.^{1,2,8–10} They developed artificial antenna systems built by sophisticated arrangements of different dyes in zeolite L. Light falling onto the dye molecules in the zeolite channels is absorbed and the energy is transported by the dye molecules via the Förster energy-transfer mechanism. Zeolite-dye host–guest systems were designed consisting of pyronine (donor) and oxonine (acceptor) dyes placed within the channels and a stopcock molecule at the end of the channels to improve the functionality of the artificial antenna systems.

Relatively little is known about the alignment of the dye molecules in the zeolite frameworks, but a detailed structural characterization is of great importance for the understanding of the functionality of photochromic host–guest systems. The

* Corresponding authors. E-mail: petra.simoncic@krist.unibe.ch, thomas.armbruster@krist.unibe.ch.

[†] University of Bern.

[‡] Swiss Norwegian Beamline.

arrangement of molecules within the zeolite framework is defined by the free aperture of the channels (dimensions of $\sim 6\text{--}8\text{ \AA}$ for 12-membered rings) as well as by the size and shape of the molecules. The molecules can be divided in three groups: (1) molecules small enough to rotate freely within the zeolite channels. (2) Middle-sized molecules for which it is difficult to predict how they arrange within the channels. (3) Long molecules, which align along the channel axis. Rather bulky molecules can only be encapsulated into very large cages, as they exist in the zeolite faujasite or in mesoporous materials. Structural arrangement and localization of photochromic dyes in zeolites are mainly investigated by optical microscopy, fluorescence microscopy, and X-ray diffraction methods.

Caro et al.⁴ presented several methods for defining the positions of two different neutral guest molecules in $\text{AlPO}_4\text{-5}$. Nanoporous $\text{AlPO}_4\text{-5}$ possesses a one-dimensional channel system running along the c -axis and forms hexagonal, elongated crystals. The arrangement of these molecules was tested by optical microscopy, Raman spectroscopy, second-harmonic generation, and pyroelectric studies. On the basis of the results of these different methods, the authors postulated a preferred orientation of the guest molecule along the channel axis.

Megelski et al.¹⁰ derived a relationship between the orientation of cationic oxonine and pyronine in zeolite L and emitted light intensity recorded by polarized fluorescence microscopy. Cone-shaped distributions of the transition-dipole moment were defined for these two molecules with a cone-half-angle of 30° for pyronine and 40° for oxonine, indicating a significant rotational disorder within the channel cross section.

Alvaro et al.¹¹ encapsulated the photoluminescent polyphenylenylylene oligomer (PPV) into zeolite X and Y by in-situ polymerization. The organic oligomers inside the zeolites were characterized by diffuse reflectant UV-vis, IR, and MAS ^{13}C NMR spectroscopy. The stability of PPV in zeolite X and Y is clearly enhanced so that this system can be used for laser flash photolysis.

Structural studies of dye-zeolite guest-host systems by X-ray diffraction are relatively rare. Van Koningsveld et al.¹² describe the positions of p -xylene in the 10-membered ring channels of zeolite H-ZSM-5. P -xylene was incorporated by gas phase and subsequently analyzed by applying single-crystal X-ray diffraction. The authors reported a change in space group compared to the pure H-ZSM-5 phase and located two different preferred orientations of the p -xylene molecule within the ZSM-5 channel system.

Hoppe et al.⁶ investigated the incorporation of methylene blue into zeolite NaY by powder X-ray diffraction. They compared two different incorporation methods (ion-exchange, crystallization inclusion) resulting in two different preferred positions within the large cages of zeolite Y. Furthermore, they observed also a striking influence of the dye on the Na distribution.

Hennessy et al.¹³ characterized the arrangement of methyl viologen (MV^{2+}) in zeolite L. They combined powder X-ray diffraction, IR, and Raman spectroscopy and molecular modeling to localize the molecule within the framework. Because of the shape and size of the molecule and the aperture of the channels of zeolite L, they postulated a slightly inclined orientation of the molecule along the channel axis. In addition, they used the zeolite framework vibrations recorded by IR and Raman spectroscopy as an internal standard for a nondestructive method to determine the degree of dye loading.

Probably the first example of a composite material consisting of a silicate host and an organic guest (indigo) is Maya blue, first produced in the eighth century by the Mayas in Mexico.

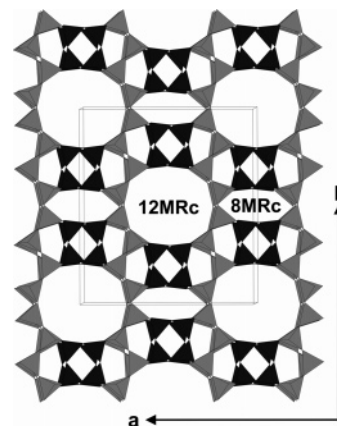


Figure 1. Tetrahedral framework structure of mordenite with unit cell outlines. The structure can be envisioned as built by puckered sheets (light gray shading) parallel to (100) formed by six-membered rings of tetrahedra. These sheets are connected along a by four-membered ring pillars (dark gray shading) in a way that 12-membered ring channels (12MRc) and compressed eight-membered ring channels (8MRc) are formed, both extending along c .

Using powder X-ray diffraction and molecular modeling, Chiari et al.¹⁴ investigated the synthetic pigment Maya blue, a combination of the clay mineral palygorskite and the organic dye indigo. Palygorskite possesses large channels with free dimensions of $7.3 \times 6.3\text{ \AA}$ in which the dye molecule fits without steric impediments. The authors describe a formation of strong hydrogen bonds between the $\text{C}=\text{O}$ group of the molecule and structural H_2O of the clay. Furthermore, they observed a sixfold disordered arrangement of the indigo molecule within the clay channels.

In this study, mordenite was chosen for the structural study of incorporated thionin blue because of the slightly oblate cross section of the large twelve-membered ring channels. In combination with the relatively low symmetry of mordenite (pseudo-orthorhombic), the oblate cross section of the channels suggested a more anisotropic orientation of the molecule compared to hexagonal zeolites, such as zeolite L. In hexagonal zeolites, the main channels run parallel to the sixfold axis, and molecular disorder is therefore already predetermined by the symmetry of the tetrahedral framework.

The structure of mordenite possesses large, ellipsoidal 12-membered ring channels (12MRc: free aperture $7 \times 6.5\text{ \AA}$) and compressed eight-membered ring channels (8MRc: free aperture $5.7 \times 2.6\text{ \AA}$) parallel to the c -axis (Figure 1). These channels are connected by another set of compressed eight-membered ring channels parallel to the b -axis.¹⁵⁻¹⁷

The mordenite structure at room temperature is usually refined in space group $Cmcm$ or $Cmc2_1$, respectively.^{15,18} Simonic and Armbruster¹⁹ proposed a domainlike structure where about 3% of the Si/Al framework is shifted by $c/2$. Despite these studies, the symmetry of the framework is generally handled as pseudosymmetry and represents only a fair approximation. Lower symmetries or microtwin models are also proposed²⁰ but not proven by experiments. As already shown in the structure refinement of pure mordenite-Na and a selenium-modified mordenite-Na at 120 K,²¹ the monoclinic space group Cc was used as a "best fit" for the agreement between structure model and diffraction data.

Mordenites are divided into two groups: (1) large port mordenites, which can absorb molecules $>4.5\text{ \AA}$, and (2) small port mordenites, which can absorb only molecules $<4.5\text{ \AA}$.²² The large port character of the mordenite crystals used in this

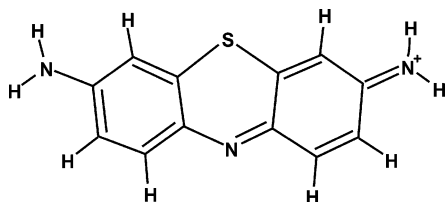


Figure 2. Cationic thionin molecule ($C_{12}H_{10}N_3S^+$). The planar organic molecule ($7.2 \times 15 \text{ \AA}$) fits into the large 12-membered ring channel of mordenite

study has already been confirmed by the incorporation of Se chains with a length up to 10 \AA .²¹

Cationic thionin blue ($C_{12}H_{10}N_3S^+$), which was used for dye incorporation, is a sulfur-containing, single-charged, flat molecule with dimensions of $7.2 \times 15 \text{ \AA}$ on the basis of van der Waals radii (Figure 2).

The focus of this single-crystal X-ray study is the characterization of the arrangement of cationic thionin blue within the channels of the zeolite mordenite. The large ellipsoidal 12-membered ring channels along [001] with free aperture of $7 \times 6.5 \text{ \AA}$ are tailor-made for incorporation of small organic dyes. Furthermore, the charge distribution on the internal walls of the zeolite channels may influence the orientation of the trapped molecules.

Experimental Section

Crystal Synthesis. Pure mordenite–Na crystals were synthesized hydrothermally in the home lab after a modified method by Warzywoda et al.²³ The exact synthesis conditions are reported in Simoncic and Armbruster.^{19,21} The crystallization products were 100% mordenite with platy and uniform morphology. The run products were studied with a polarizing microscope and the single crystals were examined with a scanning electron microscope and showed well-defined, but slightly curved, faces and no apparent twinning. Average size of the mordenite crystals was about $0.06 \times 0.04 \times 0.05 \text{ mm}$.

Dye Incorporation. Self-synthesized mordenite–Na was used for encapsulation of cationic thionin blue. Dye incorporation was carried out by ion exchange. Pure mordenite–Na single crystals (0.5 g) were treated in $8 \times 10^{-2} \text{ M}$ aqueous thionin–acetate solution ($C_{12}H_9N_3S \times C_2H_4O_2$, Aldrich, 90%) at $95 \text{ }^\circ\text{C}$ for 6 weeks in a sealed Teflon vessel. The stability of thionin blue in aqueous solution at boiling temperature was demonstrated experimentally by Calzaferri et al.²⁴ In our experiment, the dye solution was renewed every week. After ion exchange, crystals were extensively washed with distilled water and hydrochlorite solution (14%, Hanseler) to remove adsorbed molecules from the crystal surface.

For geometrical reasons, the dye loading in the mordenite structure cannot exceed one molecule per formula unit. The periodicity of the mordenite c translation (7.5 \AA) corresponds to the half-length of the molecule (15 \AA). With two 12-membered ring channels per unit cell, this results in complete filling for one molecule per formula unit. Thionin-loaded mordenite was quantitatively determined by electron microprobe analyses resulting in the composition $Na_{5.5}Thionin_{0.4}Si_{42.02}Al_{5.88}O_{96} \times nH_2O$, where the S-concentration was taken as measure of the thionin content.

Furthermore, dye-loaded mordenite single crystals were investigated with plane-polarized light using an optical microscope determining the pleochroism, which is indicative of the orientation of the transition-dipole moment of the dye molecule.

X-ray Data Collection. X-ray data collection of synthetic mordenite–Na (as synthesized) and thionin blue-treated (thio-

TABLE 1: Experimental Parameters for X-ray Data Collection and Refinement of Mordenite–Na²¹ and Thionin–Mordenite–Na

sample	mordenite–Na	thionin–mordenite–Na
crystal size (mm)	0.05 0.04 0.05	0.06 0.05 0.03
diffractometer	MAR image plate	MAR image plate
X-ray radiation	synchrotron (0.79946 \AA)	synchrotron (0.80000 \AA)
temperature	120 K	120 K
space group	Cc	Cc
cell dimensions (\AA)	18.073(3), 20.463(3), 7.5145(9)	18.126(3), 20.403(2), 7.499(1)
β ($^\circ$)	90.05(1)	90.02(2)
absorption corr.	sadabs	sadabs
maximum 2θ	55.13	58.53
measured reflections	15595	18616
index range	$-20 \leq h \leq 20$, $-23 \leq k \leq 23$, $-8 \leq l \leq 8$	$-22 \leq h \leq 22$, $-24 \leq k \leq 24$, $-9 \leq l \leq 9$
unique reflections	4468	5205
reflections $> 4\sigma(F_o)$	4180	4564
R_{int}	0.0347	0.0390
R_σ	0.0398	0.0350
number of l.s. parameters	362	373
Goof	1.131	1.127
$R1, F_o > 4\sigma(F_o)$	0.0525	0.0549
$R1, \text{all data}$	0.0573	0.0621
wR2 (on F_o^2)	0.1095	0.1441

nin–mordenite–Na) single crystals was performed at 120 K using a conventional N_2 gas cooling device (Oxford cryosystems) and synchrotron radiation (wavelength $\lambda = 0.79946 \text{ \AA}$ for mordenite–Na, $\lambda = 0.80000 \text{ \AA}$ for thionin–mordenite–Na) on the single-crystal diffraction line at SNBL (ESRF, Grenoble) where diffracted intensities were registered with an MAR image plate. Wavelengths for both measurements were calibrated against a reference Si powder sample. The double experiments were performed to detect possible phase transitions in the mordenite structure at low temperature because of the influence of thionin incorporation. The reason for intensity data collection at low temperature was to reduce thermal vibration of extraframework dye molecules to allow more accurate localization. The diffraction data did not reveal diffuse features or superstructure reflections as could have been expected because of the relation between the periodicity of the mordenite c translation (7.5 \AA) and the length of the molecule (15 \AA). Data reduction was performed with the program package CrysAlis²⁵ and an empirical absorption correction was made with Sadabs.²⁶ A summary of experimental parameters is given in Table 1.

Structure refinement for mordenite–Na and thionin–mordenite–Na was carried out with the program SHELXL97,²⁷ using neutral-atom scattering factors (Si for all tetrahedral sites—labeled T sites). Refinements were performed with anisotropic displacement parameters for all framework sites. Previous structure refinement of pure mordenite–Na and Se-modified mordenite–Na at 120 K suggested space group Cc as an appropriate model, because it led to a proper description of the tetrahedral framework.²¹ Therefore, final data for thionin–mordenite–Na were also refined in this space group. In addition, a $c/2$ -shifted defect domain was introduced and fully constrained to the Si/Al framework.^{19,21} Coordinates of tetrahedral sites showing strong correlations were constrained to each other (Table 3S). Na- and H_2O positions were determined by comparison with diffraction data of synthetic mordenite at room temperature, analyzing interatomic distances and difference

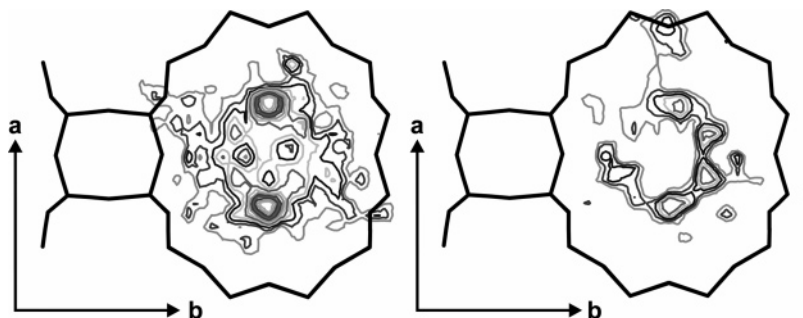


Figure 3. Difference Fourier maps of thionin–mordenite–Na and mordenite–Na, contours at 0.1 electron interval for both maps. Left: thionin–mordenite–Na, (001) section of the 12-membered ring channel at $z = 0.90$. Strong peaks shifted $\pm x$ from the center of the channel indicate the position of sulfur atoms whereas smeared electron density around the center of the channel is characteristic of the thionin molecule. Right: mordenite–Na, (001) section of the 12-membered ring channel at $z = 0.90$. Electron density around the center of the large 12-membered channel is due to H_2O molecules.²¹

Fourier maps.¹⁹ Thionin-molecule sites were determined comparing the difference Fourier maps of the large 12-membered ring channel with corresponding electron density of the pure mordenite–Na. More details about the refinement of the Si, Al framework of mordenite–Na at 120 K can be found in Simoncic and Armbruster ref.²¹

Results

Structure of Thionin–Mordenite–Na. The unit cell of the thionin-modified sample shows a clear expansion of the a -axis and a shortening of the b -axis because of the incorporation of the flat organic molecule. Mean T–O bond lengths of thionin–mordenite–Na show within two standard deviations the same T–O distances as for pure mordenite–Na at 120 K.²¹

Because of geometrical and space-filling considerations, the thionin molecule can only be incorporated into the large 12-membered ring channel. Molecule sites were identified by analyzing the difference Fourier map. The position of thionin can be best located by determining the position of the sulfur atom, because it has the largest scattering factor within the organic molecule. The sulfur sites are clearly detectable on the difference Fourier map within the larger 12-membered channel along the c -axis (Figure 3). The electron density of the thionin-loaded mordenite shows distinct peaks shifted $\pm x$ from the center of the 12-membered ring channel. These peaks were not found in the electron density map of the pure Na–mordenite but a weaker electron density distribution around the center of the channel is visible indicating disordered H_2O molecules in mordenite–Na.¹⁹

Four different, partly occupied thionin sites are oriented slightly inclined along the channel axis (Figure 4). Two molecule sites were located at opposite positions at $x \approx \pm 0.1$ and $z \approx 0$, and the other two at $x \approx \pm 0.1$ are separated by $c/2$ at $z \approx \pm 0.25$ (Figure 5). Because the electron density peaks within the 12-membered ring channel indicated distinct disorder, the nearest neighbor and next-nearest neighbor distances within the molecule were fixed during the refinement using bond lengths reported for methylene blue²⁸ and were optimized with Chem-Sketch structure package.²⁹ S–C nearest-neighbor distances were fixed to 1.73–1.74 Å, C–C distances to 1.35–1.49 Å, and N–C distances to 1.30–1.40 Å. All molecules were constrained to flat geometry. The population of individual atoms was constrained to be equal within one molecule. Isotropic displacement parameters for the sulfur atoms were free during the refinement whereas the displacement parameters of C- and N-atoms were fixed. Positions and isotropic displacement parameters of H-atoms were not determined.

The shortest S \cdots O distance (2.97(1) Å) was determined between the sulfur atom of molecule A (S1a) and channel wall oxygen O7b whereas the shortest N \cdots O distance is between N3b (molecule B) \cdots O5b and N3d (molecule D) \cdots O3b, both yielding 3.04(1) Å. The shortest C \cdots O distance (3.11(1) Å) is between C9c (molecule C) and O7b. Other short C \cdots O and N \cdots O distances and population parameters for each molecule are summarized in Table 2.

In the large 12-membered ring channel, besides the dye molecules, five H_2O sites and only one Na site were found. Two H_2O sites (population 0.2–0.5) were found in the center of the channel shifted along the b -axis, another set of H_2O molecules (population 0.21–0.34) sites were also close to the center of the channel but shifted along the a -axis. One Na site (Na3, population 0.16) was also located in the center of the channel shifted along the b -axis. At the intersection between the large 12-membered channel and the eight-membered ring channel along the b -axis, as well as within the 8MR channel along b , additional H_2O and Na sites were found. Three Na sites (Na2, population 0.20; Na6, population 0.22; Na7, population 0.15) are close to the cross section of the 12MRc and 8MRb. Na3 (population 0.15) and Na4 (population 0.16) are close to the intersection of 8MRb and 8MRc. Another two H_2O molecules are in the eight-membered ring channel along b . In the compressed eight-membered channel along the c -axis, Na1 (population 0.16) is coordinated by a highly populated H_2O site (population 0.5). The results of the structure refinement, including atomic coordinates, populations, and isotropic displacement parameters are given in Table 3S (Supporting Information) for the thionin–mordenite–Na sample.

Optical Microscopy. Striking pleochroism phenomena of the dye-loaded mordenite single crystals were observed by optical microscopy using plane-polarized light. In Figure 6a–d, the crystal orientation is indicated by the direction of the cell axes. Polarization direction is shown by a double-headed arrow. Figure 6a and b shows the (100) face of the mordenite crystal. The crystal appears dark blue if the polarization direction is parallel to the c -axis (Figure 6a), whereas the crystal is only light blue if the polarization direction is parallel to the b -axis (Figure 6b). Figure 6c and d displays the (001) face of the crystal, a section perpendicular to the large channels. With a polarization direction parallel to the a -axis, the crystal appears purple, while a polarizer orientation parallel to the b -axis shows a blue crystal.

These observations can be interpreted by the orientation of the thionin molecule's transition-dipole moment, which runs along the molecule's long axis.¹⁰ If the electric field of polarized light is oriented parallel to the transition-dipole moment (Figure 6a), light is absorbed by the dye molecule and the crystal appears

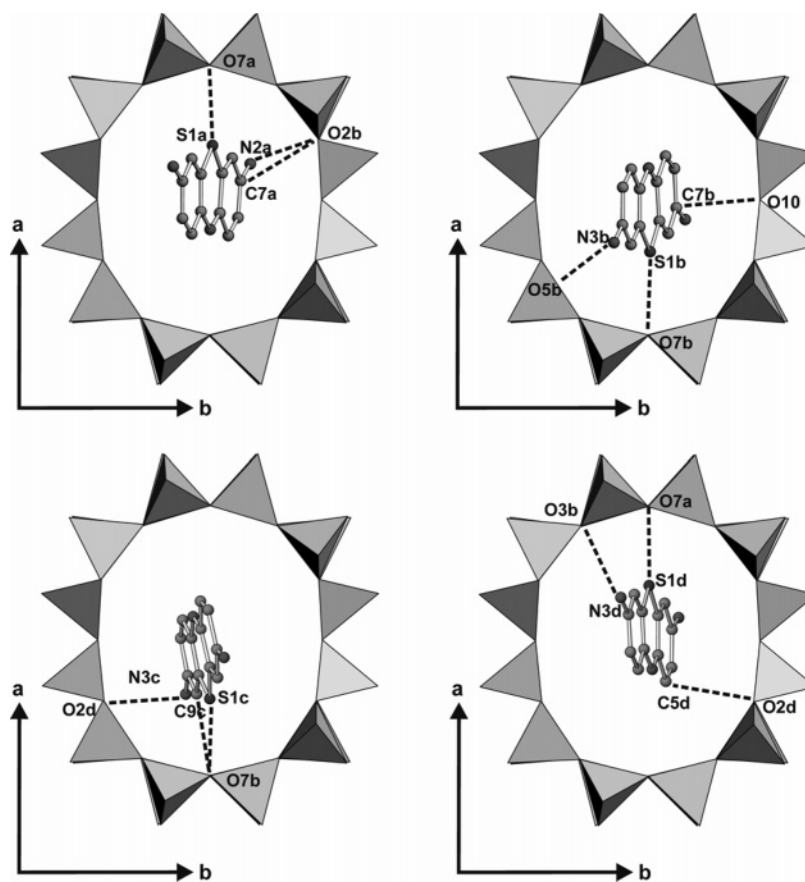


Figure 4. Thionin molecule sites within the large 12-membered ring channel showing inclined orientation within the channel cross section. Shortest $S\cdots O$, $C\cdots O$, and $N\cdots O$ distances from the molecules to the channel wall oxygens are indicated by dashed lines. H-atoms are not displayed.

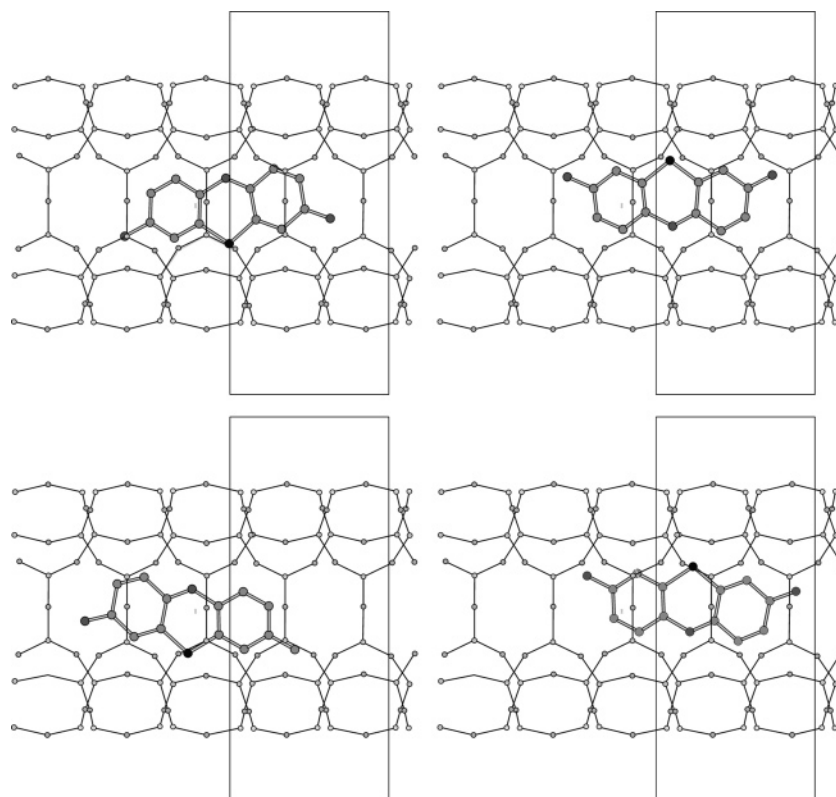


Figure 5. Thionin molecule sites within the large 12-membered ring channel along c . Unit cell dimensions are indicated by rectangles. Black dots represent the sulfur atom. Upper row: Molecules at $x \approx \pm 0.1$ and $z \approx 0$. Lower row: $x \approx \pm 0.1$ and $z \approx \pm 0.25$.

blue. On the other hand, the crystal appears only light blue if the polarization direction is parallel to the b -axis (Figure 6b).

This indicates that the dye molecules within the channel are not exactly aligned parallel to the channel axis but inclined

TABLE 2: Shortest S···O, C···O, and N···O Distances from the Thionin Molecule to the Channel Wall Oxygens^a

S···O distances		shortest N···O distances	
S1a–O7a	2.97(1) Å	N2a–O2b	3.07(2) Å
S1b–O7b	3.18(1) Å	N3b–O5b	3.04(1) Å
S1c–O7b	3.05(2) Å	N3c–O2d	3.20(1) Å
S1d–O7a	3.12(1) Å	N3d–O3b	3.04(1) Å

shortest C···O distances		molecules per formula unit	
C7a–O2b	3.27(1) Å	molecule A	0.045(8) pfu
C7b–O10	3.20(2) Å	molecule B	0.207(9) pfu
C9c–O7b	3.11(1) Å	molecule C	0.098(6) pfu
C5d–O2d	3.36(1) Å	molecule D	0.042(8) pfu

^a Concentrations are given in units per formula.

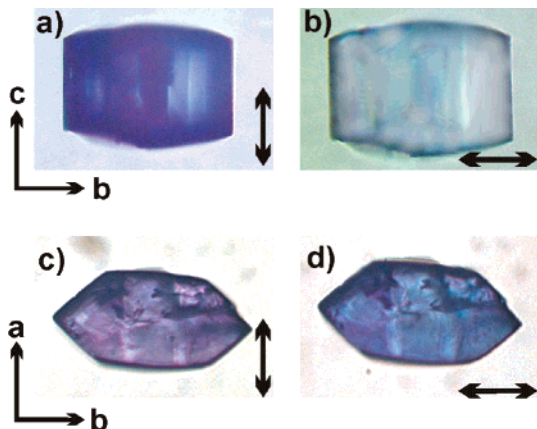


Figure 6. Optical micrographs of a dye-loaded mordenite single crystal under plane-polarized light. 6a and b: (100) of the crystal. Crystal orientation is envisioned with the unit cell axes, polarization direction with double-headed arrows. 6a shows a dark blue crystal under plane-polarized light parallel to the *c*-axis, 6b shows the same crystal with plane-polarized light parallel to the *b*-axis appearing only light blue. 6c and d show a section perpendicular to the large channels (001) face). Polarization direction parallel to the *a*-axis shows a purple crystal, parallel to the *b*-axis a blue crystal.

regarding the channel cross section. This assumption is also confirmed by the pleochroism observed in the crystal section perpendicular to the large channels (Figure 6c and d). Light is also absorbed by the organic molecules in this alignment (blue, purple), which is only possible if the molecules are inclined within the channel cross section. If the molecules were arranged exactly upright in the channel, no light would be absorbed in this orientation and the crystal would appear colorless. In addition, the color change from blue to purple indicates a nonrandom orientation of the dyes within the channel cross section.

Corresponding phenomena can be observed by fluorescence microscopy of dye-loaded mordenite single crystals using plane-polarized light (Figure 7a–d). Fluorescence of the thionin molecules was excited using light from a 100 W mercury lamp passed through a U-MWIY excitation cube (wavelength 545–580 nm). Excited dye-loaded mordenite single crystals emitted red light. The same crystal and polarization directions as for optical microscopy were applied, showing also anisotropic behavior of light emission. Intense red fluorescence is emitted if the polarization direction is parallel to the *c*-axis whereas only very weak intensity appears if the polarization direction is parallel to the *b*-axis (Figure 7a and b, (100) orientation of the mordenite crystal). A difference in the fluorescence intensity is also observed at the (001) crystal orientation (Figure 7c and d): a polarization direction parallel to the *a*-axis shows slightly

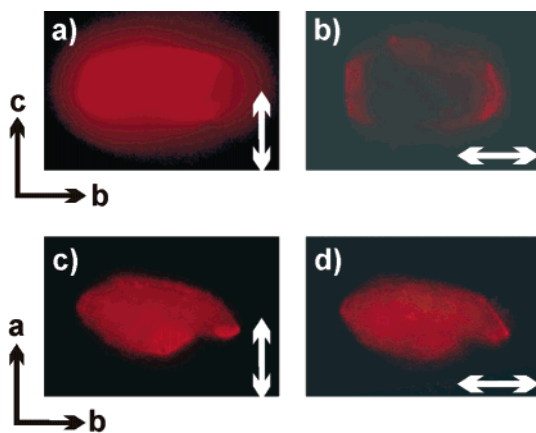


Figure 7. Fluorescence microscopic pictures of thionin-loaded mordenite single crystals, excitation at 545–580 nm. 7a and b display the (100) crystal face. 7a shows intense light emission with polarization direction parallel to the *c*-axis. 7b shows only very weak emission with polarization direction parallel to the *b*-axis. 7c and d show a section perpendicular to the large channels. The polarization direction parallel to the *a*-axis shows more intense light emission (Figure 7c) than with the polarizer parallel to the *b*-axis (Figure 7d).

more intense light emission (Figure 7c) than with a polarization direction parallel to the *b*-axis (Figure 7d). The appearance of anisotropic fluorescence phenomena can be explained by the orientation of the transition-dipole moment of the thionin molecule as it was derived from the optical-microscopy experiments.

Discussion

The Mordenite Framework. Application of low temperature (120 K), chosen for an improved resolution of extraframework occupants and dye molecules, led also to a better resolution of the complex disordered microstructure within the tetrahedral framework. One has to assume that the refinement in space group *Cc* does not express the true framework symmetry because lower symmetry or microtwin models, as proposed by Gramlich–Meier,¹⁸ cannot be ruled out. Mordenite–Na, Se–mordenite–Na,²¹ as well as thionin–mordenite–Na have the same space group *Cc* in common; thus a phase transition caused by dye incorporation can be excluded.

Extraframework Atoms. Extraframework Na and H₂O distribution of the thionin-loaded mordenite–Na is highly influenced by the incorporation of the organic molecule. By comparison with diffraction data of pure mordenite–Na (Figure 8, 9),²¹ two points are remarkable: (1) the population of the Na sites is more uniformly distributed than in pure mordenite–Na, and (2) the large 12-membered ring channel is much less populated by Na than in pure mordenite–Na. It is striking that the Na1 site in the compressed eight-membered ring channel along the *c*-axis is populated with only 0.64 Na per formula unit (pfu) whereas this site is highly populated in mordenite–Na (2.28 Na pfu). In contrast, additional Na sites (Na4, Na5, Na6, Na7) within the eight-membered ring channel along the *b*-axis were found, which do not occur in the pure mordenite–Na sample. As the organic thionin molecule is incorporated in the large 12-membered ring channel, there are remarkable differences between the Na and H₂O extraframework distribution in the thionin–mordenite–Na and pure mordenite–Na. In mordenite–Na, 2.72 Na pfu was found in the large 12-membered ring channel along the *c*-axis whereas in the thionin–mordenite–Na only 0.64 Na pfu is located in this channel. Because the incorporation of cationic thionin blue is based on

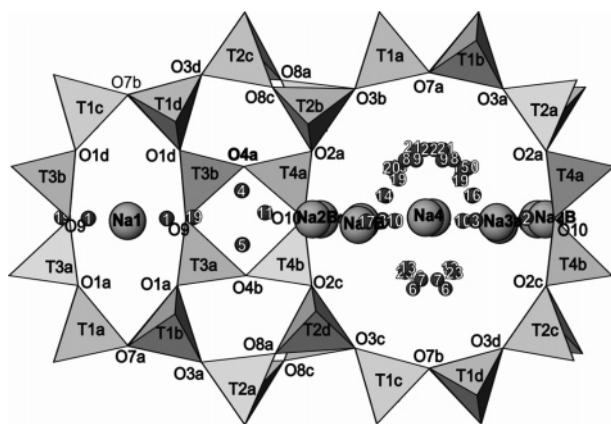


Figure 8. Extraframework cation and H₂O molecule positions in mordenite–Na. Small circles with numbers correspond to H₂O positions. Compare H₂O positions with electron density in Figure 3.

ion exchange, part of the Na ions in the 12-membered ring channel were replaced or shifted toward the eight-membered ring channels along the *b*-axis, providing space for the entering organic molecule. Both the chemical analysis by electron microprobe and the structure refinement yielded about 0.4 thionin molecules per formula unit. To maintain charge balance this requires about 5.5 Na pfu, but in the structure refinement only 4.8 Na pfu was determined. This discrepancy can be explained by a more random distribution of the Na sites within the mordenite channels. Although only 0.4 Na pfu was replaced by thionin⁺, the entire Na distribution is influenced by the dye incorporation because the large 12-membered channels are filled by the large molecule which forces the extraframework cations to relocate at new positions.

In addition, the distribution of the H₂O molecules is influenced by the dye incorporation. Compared to 26 H₂O pfu in the pure mordenite–Na, only 10 H₂O pfu is present. In particular, only 6.5 H₂O pfu remained in the 12-membered ring channel of thionin-exchanged mordenite whereas 19 H₂O pfu was located in pure mordenite–Na.

Arrangement of Thionin Blue in the Mordenite Channels.

Because most studies on dye-loaded zeolites were performed on zeolites with nearly circular shaped channel cross sections (AlPO₄-5, zeolite L, zeolite Y),^{4,6,10,13} dye localization is hampered by the high, sixfold symmetry of these channels. The circular channels and the shape of the incorporated molecules do not allow a preferred orientation, and the molecules arrange more or less randomly within the channel cross section. This assumption is confirmed by fluorescence microscopy performed on dye-loaded zeolite L crystals building hexagonal, elongated columns.¹⁰ Crystals lying on the column side (incident light perpendicular to the channel axis) showed anisotropic light emission upon changing of the polarization direction whereas crystals standing on the hexagonal end faces (incident light parallel to the channel axis) displayed radial distribution of light emission. This suggests that the transition-dipole moment of the dye molecules are fanned out radially perpendicular to the channel axis, and the molecules are not arranged in a preferred orientation.

The choice of a thionin–mordenite guest–host system should simplify the structural characterization and dye localization in two ways. (1) The anisotropic, ellipsoidal shape of the large 12-membered ring channel forces the molecule to arrange in a more ordered way. (2) The relatively heavy sulfur atom of the thionin-molecule is easily located by analyzing the difference Fourier map. In contrast, most studies mentioned above used

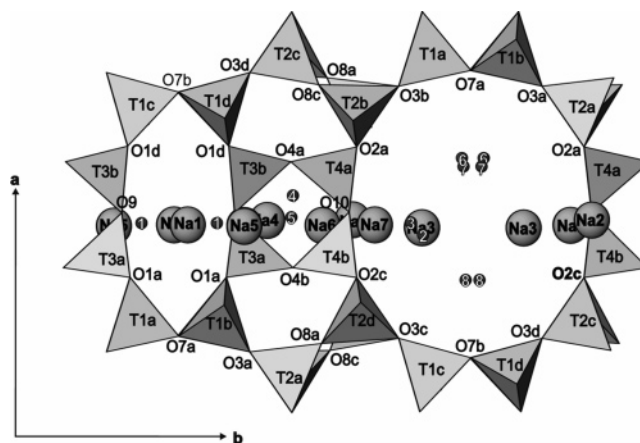


Figure 9. Extraframework cation and H₂O molecule positions in thionin–mordenite–Na. Small circles with numbers correspond to H₂O positions. Thionin molecule positions are not displayed. Note the Na sites shifted to the eight-membered ring channel along the *b*-axis, which do not appear in mordenite–Na.

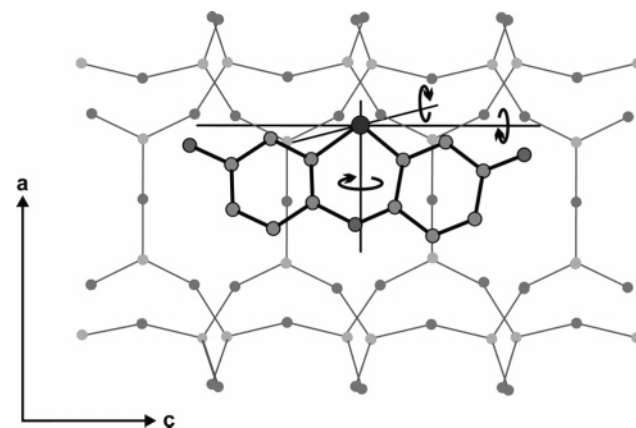


Figure 10. Thionin molecule within the large 12-membered ring channel long the *c*-axis. H-atoms are not shown. Possible rotation directions of the molecule are envisioned by a coordinate system with origin in the S-atom and axes parallel to the unit cell axes.

dye molecules consisting of C, N, and O, which are more difficult to localize in the relatively heavy matrix of a zeolite.

On the other hand, because of the shape and the size of the thionin molecule, a slight rotational disorder of the molecule within the channel cross section has to be expected. Because the position of the sulfur atom can be assumed as well defined, as it was obvious from the difference Fourier map, the molecule can rotate around three axes defining a coordinate system with the S-atom as a center and axes parallel to the crystal's unit cell dimensions (Figure 10).

This rotational disorder within the large 12-membered channels can be quantified using the minimum C···O (channel wall) and N···O distances. In a *p*-xylene loaded ZSM-5,¹² C···O distances from 3.16 to 3.68 Å were determined. Studies of interactions between CH-groups and H₂O molecules showed C···O distances around 3.3 Å.³⁰ Furthermore, N···O distances between NH₄⁺ ions and the cavity walls of the zeolite heulandite are 3.0 Å.³¹ These reported distances are in good agreement with C···O and N···O distances yielded in this study, which are between 3.1 and 3.36 Å for C···O and 3.04–3.2 Å for N···O, respectively. Therefore, taking these minimum distances (C···O: 3.1 Å and N···O: 3 Å) into account, a rotation of the molecule (librational disorder) is limited. In particular, molecule positions with the molecule's long axis parallel to the *a*-axis and *b*-axis are not possible. Furthermore, a molecule orientation

with the molecule's long axis parallel to the *c*-axis but with the molecule's plane parallel to (100) is not possible. Applying the AmiraMol visualization package,³² a maximum rotation of the molecule of about 12° in each direction with sulfur as a center of the abovementioned coordinate system seems possible.

The molecule–framework distances are shorter than the sum of the van der Waals radii, suggesting electrostatic interaction between the molecule and the zeolite framework. The short C···O and N···O distances point to presence of relatively strong CH···O and NH···O hydrogen bonds, which is supported by the structural study of methyl viologen in zeolite L.¹³ Finally, one can assume that the molecule prefers an inclined position within the channel cross section because this results in the formation of stronger hydrogen bonding to the framework. In contrast, a hypothetical perfectly centered and upright orientation of the molecule along the channel axis results in a C···O distance of 3.8 Å and a N···O distance of 3.88 Å suggesting considerably softer bonding to the framework than observed for the inclined orientation.

The refined inclined arrangements of the thionin molecules are in good agreement with the observations made by optical and fluorescence microscopy. Appearance of light absorption and pleochroism observed at incident plane-polarized light parallel to the channel axis can only be explained by an inclined arrangement of the dye molecule within the 12-membered ring channel. Furthermore, the pleochroic change from blue to purple indicates a partially ordered, nonrandom orientation of the dye within the channel cross section.

In addition to the rotational disorder within the channel cross section, there is also occupational disorder along the channel axis, which means that the four resolved sites of dye molecules are statistically occupied. This is supported by the nonobserved diffuse features or superstructures in the diffraction data. Taking into account that the length of the molecule is twice the periodicity of the *c*-axis, the dye loading of 40% and missing superstructure reflections as well as nonobserved diffuse scattering features indicate that the dye molecules are randomly anchored to specific framework sites.

The incomplete filling (ca. 40%) of the large mordenite channels with thionin may be explained by the applied temperature for dye incorporation. Dye incorporation at 95 °C suggests under these conditions strong dynamic translational and librational disorder of the dye molecules, leading to mutual repulsion of the cationic dye molecules along the channel axis. This dynamic disorder was not observed in the X-ray experiment because the molecules were “frozen” at 120 K at energetically preferred channel sites. Nevertheless, significant disorder (librational and occupational) has been found for the four resolved dye-molecule orientations.

It has been shown for zeolite L that higher dye loading could be achieved if the dye-incorporation experiments were carried out at room temperature.^{13,33} On the other hand, zeolite L crystals were about 1 order of magnitude smaller (particle size 0.2–0.5 μm) than the crystals used in this study (particle size 60 μm). Thus, room-temperature exchange was possible because of the shorter diffusion pathways. Ion exchange of thionin⁺ for 6 weeks at 95 °C reached equilibrium condition because no color or chemical zoning was detected parallel to the zeolite channel axis (Figures 6a and 7a).

We showed that the structural study of organic dyes in a zeolite with an oblate channel cross section simplifies the localization of the guest molecule and gives new insight into guest–host framework interactions. Single-crystal X-ray diffraction represents a powerful tool for a detailed characterization

of guest–host systems and completes methods such as IR, Raman, or fluorescence spectroscopy also applied for guest localization in zeolites.

Acknowledgment. This study was supported by the Swiss “Nationalfond”, credit 20-65084.01 to T. Armbruster. P. Simoncic thanks the International Center for Diffraction Data (ICDD) for a 2004 Ludo Frevel Crystallography Scholarship. We acknowledge the European Synchrotron Radiation Facility for provision of synchrotron radiation facilities and we would like to thank V. Dmitriev and S. Capelli for assistance in using the Swiss Norwegian Beam line 1A. Furthermore, we would like to thank Prof. Gion Calzaferri for the inspiring ideas and helpful suggestions. We thank E. Gnos for chemical analyses with the electron microprobe, B. Frey for crystal images by SEM, and Olivia Bossart for help with the fluorescence microscope. The authors thank two anonymous reviewers for their constructive comments.

Supporting Information Available: Atomic coordinates and B_{eq} values for synthetic thionin–mordenite–Na. This material is available free of charge via the Internet at <http://pubs.acs.org>.

References and Notes

- Calzaferri, G. *Chimia* **2001**, *55*, 1009–1013.
- Calzaferri, G.; Pauchard, M.; Maas, H.; Huber, S.; Khatyr, A.; Schaafsma, T. *J. Mater. Chem.* **2002**, *12*, 1–13.
- Braun, I.; Bockstette, M.; Schulz-Ekloff, G.; Wöhrle, D. *Zeolites* **1997**, *19*, 128–132.
- Caro, J.; Marlow, F.; Wüst, M. *Adv. Mater.* **1994**, *6*(5), 413–416.
- Ihle, G.; Schüth, F.; Kraus, O.; Vietze, U.; Laeri, F. *Adv. Mater.* **1998**, *10*(14), 1117–1119.
- Hoppe, R.; Schulz-Ekloff, G.; Wöhrle, D.; Kirschhock, C.; Fuess, H.; Uytterhoeven, L.; Schoonheydt, R. *Adv. Mater.* **1995**, *7*(1), 61–64.
- Onida, B.; Bonelli, B.; Lucco-Borlera, M.; Flora, L.; Otero Areal, C.; Garrone, E. *Stud. Surf. Sci. Catal.* **2001**, *135*, 364.
- Maas, H.; Calzaferri, G. *The Spectrum* **2003**, *16*(3), 18–23.
- Devaux, A.; Minkowski, C.; Calzaferri, G. *Chem. Eur. J.* **2004**, *10*, 2391–2408.
- Megelski, S.; Lieb, A.; Pauchard, M.; Drechsler, A.; Glaus, S.; Debus, C.; Meixner, A. J.; Calzaferri, G. *J. Phys. Chem. B* **2001**, *105*, 25–35.
- Alvaro, M.; Corma, A.; Ferrer, B.; Galletero, M. S.; Garcia, H.; Peris, E. *Chem. Mater.* **2004**, *16*, 2142–2147.
- van Koningsveld, H.; Tuinstra, F.; van Bekkum, H.; Jansen, J. C. *Acta Crystallogr., B* **1989**, *45*, 423–431.
- Hennessy, B.; Megelski, S.; Marcolli, C.; Shklover, V.; Bärlocher, C.; Calzaferri, G. *J. Phys. Chem. B* **1999**, *103*, 3340–3351.
- Chiari, G.; Giustetto, R.; Ricchiardi, G. *Eur. J. Mineral.* **2003**, *15*, 21–33.
- Meier, W. M. *Z. Kristallogr.* **1961**, *115*, 439–450.
- Meier, W. M. In *Natural Zeolites, Occurrence, Properties, Use*; Sand, L. B., Mumpton, F. A., Eds.; Pergamon: Oxford, 1978; pp 99–104.
- Armbruster, T.; Gunter, M. E. In *Reviews in Mineralogy & Geochemistry, Natural Zeolites: Occurrence, Properties, Use*; Bish, D. L., Ming, D. W., Eds.; Mineralogical Society of America: Washington, 2001, *45*, pp 1–67.
- Alberti, A.; Davoli, P.; Vezzalini, G. *Z. Kristallogr.* **1986**, *175*, 249–256.
- Simoncic, P.; Armbruster, T. *Am. Mineral.* **2004**, *89*, 421–431.
- Gramlich-Meier, R. *Strukturparameter in Zeolithen der Mordenitfamilie*. Dissertation, ETH Zürich, Nr. 6760, 1981.
- Simoncic, P.; Armbruster, T. *Microporous Mesoporous Mater.* **2004**, *71*, 185–198.
- Sand, L. B. *Synthesis of large-pore and small-pore mordenites*, Molecular Sieves, Papers of Conference, 1967; pp 71–77.
- Warzywoda, J.; Dixon, A. G.; Thompson, R. W.; Sacco, A., Jr. *J. Mater. Chem.* **1995**, *5*(7), 1019–1025.
- Calzaferri, G.; Brühwiler, D.; Megelski, S.; Pfenniger, M.; Pauchard, M.; Hennessy, B.; Maas, H.; Devaux, A.; Graf, U. *Solid State Sci.* **2000**, *2*, 421–447.
- Xcalibur System, User Manual, CrysAlis Software Package, Version 1.169*, Oxford Diffraction: Oxfordshire, U.K., 2001.

(26) Sheldrick, G. M. *SADABS*, Version 2.06; Empirical Absorption Correction Program; University of Göttingen: Göttingen, Germany, 2002.

(27) Sheldrick, G. M. *SHELX-97*; University of Göttingen: Göttingen, Germany, 1997.

(28) Marr, H. E., III; Stewart, J. M. *Acta Crystallogr., B* **1973**, 29, 847–853.

(29) *ChemSketch*, v. 5.12 (structure drawing software); Advanced Chemistry Development, Inc.: Ontario, Canada, 2001.

(30) Steiner, T. *Acta Crystallogr., D* **1995**, 51, 93–97.

(31) Yang, P.; Armbruster, T. *Eur. J. Mineral.* **1998**, 10, 461–471.

(32) *AmiraMol*, v. 3.1 (evaluation version); TGS Visual Concepts: San Diego, 2003.

(33) Calzaferri, G.; Gfeller, N. *J. Phys Chem.* **1992**, 96, 3428–3435.